Topology of structural connectomes in healthy carriers of common gene variants associated with schizophrenia

Mark Drakesmith[1,2], Thomas Lancaster[2], Sonya Foley[1,2], Lisa Brindley[1,2], Derek K Jones[1,2], and David Linden[1,2]

[1]*CUBRIC, Cardiff University, Cardiff, Wales, United Kingdom,* [2]*Neuroscience and Mental Health Research Institute, Cardiff University, Cardiff, Wales, United Kingdom*

Target Audience: Researchers and clinicians interested in using graph theory to examine psychiatric illness, particular illness risk-states.

Introduction: Understanding disconnectivity in psychiatric disorders has benefited greatly from graph theory (GT), a powerful mathematical framework that quantifies topological features of networks, beyond piecemeal analysis of network components[1]. Several previous studies have reported structural network related changes in mental illness by applying GT to tractography data[2]. However, few studies have looked at network topology as a marker for predisposition to illness[3], particularly genetic risk. In this study we examine topology of structural connectomes in healthy individuals carrying single nucleotide polymorphisms (SNPs) conferring increased risk of psychiatric disorders. The ZNF804A (rs1344706) A-allele[4] and the CACNA1C (rs1006737) G-allele[5] are two common SNPs that have been highlighted in gene-wide association studies (GWAS) to be associated with schizophrenia and bipolar disorder. This study aims to identify topological differences in carriers of these risk variants, which may contribute to mental illness.

Method: 85 neuro-typical subjects (mean age: 24.2±0.49, gender: 33/52 M/F) were scanned and genotyped. Genomic data was obtained from saliva samples. SNPs were identified using custom Ilumina SNP genotyping arrays. MRI data were acquired on a 3T GE HDx MRI system. HARDI acquisition: cardiac-gated EPI sequence, TE=87ms, 30 gradient orientations, 3 unweighted B0s, b-value=1200 smm^{-2}, FOV=96×96mm, 60 slices, voxel-size=1.6×1.6×2.4mm. HARDI data were analysed in ExploreDTI correcting the images for motion, eddy current distortions and field inhomogeneities. The Damped Lucy-Richardson algorithm[6] was used to estimate fibre orientation distributions in each voxel and streamlines estimated with deterministic tractography (2×2×2mm grid of seed points in white matter, 0.5mm step size, 45° threshold). Streamlines terminated when entering grey matter to prevent erroneous trajectories in grey matter. Tract termination points were registered to the AAL atlas, creating a 116×116 connectivity matrix. The matrices were binarised at a range of thresholds (0-25 streamlines). A range of GT metrics were computed. Network-level metrics: Global efficiency, density, mean betweenness, mean clustering coefficient, assortivity and smallworldness. Node-level metrics: degree, betweenness centrality, local efficiency, local clustering coefficient and modularity. A 1-way ANOVA was used to test for effect across the 3 genotypes for each SNP. Correction for multiple comparisons and statistical biases was carried out using multi-threshold permutation correction (MTPC)[7] (500 permutations). Regional effects on edges were also analysed using network based statistics (NBS)[8] using edges weighted by streamline density and corrected using permutation tests (5000 permutations).

Table 1. Genotype frequencies.

ZNF804A	**CC**	**AC**	**AA**
	16	31	38
CACNA1C	**GG**	**AG**	**GG**
	39	34	17

Results: Genotype frequencies for each SNP are shown in table 1. Samples for both SNPs satisfy Hardy-Weinberg equilibrium. No significant effects were found for ZNF804A. Of the network-level metrics, network density, global efficiency and mean clustering coefficient showed significant effects of CACNA1C (p_{corr}<0.05, fig. 1), all of which were higher in the non-risk genotype (GG) than in those containing the risk allele (AG and AA). Of the node-level metrics, efficiency, degree and clustering coefficient showed significant effects (p_{corr}<0.05, fig. 2). In most cases, GG was higher than the other variants, although local clustering coefficient in the inferior temporal gyrus was higher in the AA genotype. There was a significant effect on node degree in the precuneus where the AA genotype showed a significantly lower node degree compared to GG and AG genotypes. NBS results showed numerous regional network effects in short range occipital and parietal connections (fig. 3).

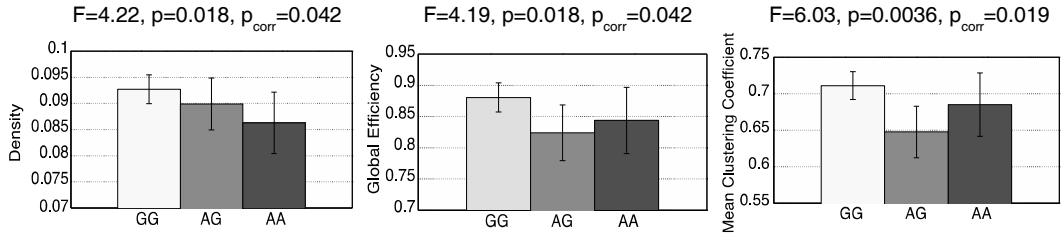

Fig. 1. Network-level GT metrics showing significant effects of CACNA1C (p_{corr}<0.05).

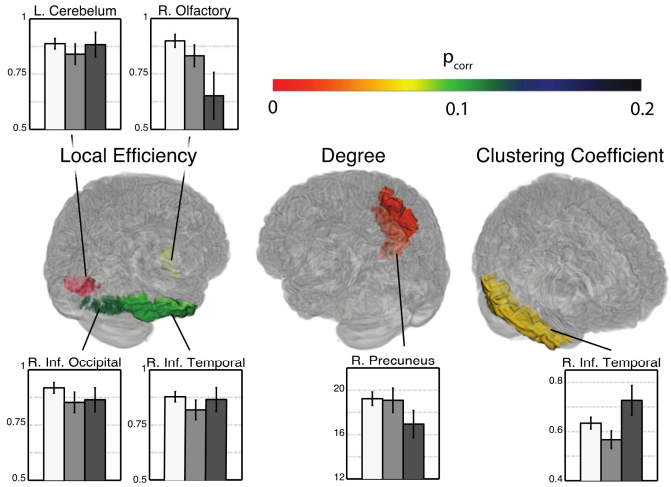

Fig. 2. Node level GT metrics showing significant effects of CACNA1C (p_{corr}<0.05).

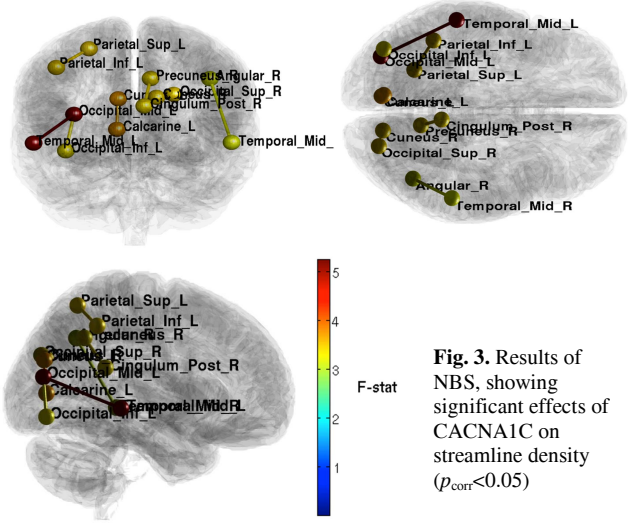

Fig. 3. Results of NBS, showing significant effects of CACNA1C on streamline density (p_{corr}<0.05)

Discussion: This is the first study to show significant differences in connectome topology of healthy individuals carrying a common genetic risk-variant associated with mental illness. Similar reductions in global efficiency, density and clustering coefficients have previously been reported in schizophrenia[9]. In particular, local topological deficits in the precuneus, a critical network hub[10] and surrounding connections suggests a degree of predisposition to functional disturbance in carriers of the risk-variant of CACNA1C. An interesting observation is a positive effect of the risk allele on local clustering in the right inferior temporal gyrus, suggesting modular specialisation of this region is altered. CACNA1C codes for Ca^{2+} ion channels, disruption of which will lead to synaptic dysfunction. This can have subsequent downstream effects on the neurogenesis of white-matter pathways, contributing to the topological differences observed here. The absence of effects of ZNF804A is most likely due to different mechanisms of expression, which do not manifest in network topology. This study shows the utility of graph theory to identify subtle but significant network alterations in at-risk states and yield insights into how network topology can predispose the brain to dysfunction.

References: 1. Bullmore, E. & Sporns, O. *Nat. Rev. Neurosci.* **10**, 186–98 (2009). 2. Griffa, A., et al. *Neuroimage* **80**, 515–26 (2013). 3.Drakesmith, M., et al. *ISMRM.* 17 (2014). 4. Girgenti, M.J., et al. *PLoS One* **7**, e32404 (2012). 5. Nyegaard, M., et al. *Mol. Psychiatry* **15**, 119–21 (2010). 6. Dell'acqua, F., et al. *Neuroimage* **49**, 1446–58 (2010). 7. Drakesmith, M. et al. *ISMRM.* 279 (2014). 8. Zalesky, A., et al. *Neuroimage* **53**, 1197–1207 (2010). 9. Van den Heuvel, M.P., et al. *J. Neurosci.* **30**, 15915–26 (2010). 10. Hagmann, P., et al. *PLoS Biol.* **6**, e159 (2008).